JOURNAL OF THE AMERICAN CHEMICAL SOCIETY

Anatolian University Libraries Consortium

Subscriber access provided by ORTA DOGU TEKNIK UNIVERSITESI KUTUPHANESI

Article

A Screening Approach for the Discovery of Mechanochromic Gold(I) Isocyanide Complexes with Crystal-to-Crystal Phase Transitions

Tomohiro Seki, Yuki Takamatsu, and Hajime Ito

J. Am. Chem. Soc., **Just Accepted Manuscript** • DOI: 10.1021/jacs.6b02409 • Publication Date (Web): 12 Apr 2016

Downloaded from http://pubs.acs.org on April 12, 2016

Just Accepted

“Just Accepted” manuscripts have been peer-reviewed and accepted for publication. They are posted online prior to technical editing, formatting for publication and author proofing. The American Chemical Society provides “Just Accepted” as a free service to the research community to expedite the dissemination of scientific material as soon as possible after acceptance. “Just Accepted” manuscripts appear in full in PDF format accompanied by an HTML abstract. “Just Accepted” manuscripts have been fully peer reviewed, but should not be considered the official version of record. They are accessible to all readers and citable by the Digital Object Identifier (DOI®). “Just Accepted” is an optional service offered to authors. Therefore, the “Just Accepted” Web site may not include all articles that will be published in the journal. After a manuscript is technically edited and formatted, it will be removed from the “Just Accepted” Web site and published as an ASAP article. Note that technical editing may introduce minor changes to the manuscript text and/or graphics which could affect content, and all legal disclaimers and ethical guidelines that apply to the journal pertain. ACS cannot be held responsible for errors or consequences arising from the use of information contained in these “Just Accepted” manuscripts.

ACS Publications

Journal of the American Chemical Society is published by the American Chemical Society. 1155 Sixteenth Street N.W., Washington, DC 20036

Published by American Chemical Society. Copyright © American Chemical Society. However, no copyright claim is made to original U.S. Government works, or works produced by employees of any Commonwealth realm Crown government in the course of their duties.

A Screening Approach for the Discovery of Mechanochromic Gold(I) Isocyanide Complexes with Crystal-to-Crystal Phase Transitions

Tomohiro Seki,*[a] Yuki Takamatsu,[a] and Hajime Ito*[a]

Division of Applied Chemistry and Frontier Chemistry Center (FCC), Faculty of Engineering, Hokkaido University, Sapporo, Hokkaido 060-8628, Japan

ABSTRACT: Mechano-induced phase transitions of emissive organic crystalline materials have received much attention. Although a variety of such luminescent mechanochromic compounds have been reported, it is challenging to develop mechanochromic compounds with crystal-to-crystal phase transitions in which precise structural information about molecular arrangements can be obtained. Here, we report a screening approach to explore mechanochromic compounds exhibiting a crystal-to-crystal phase transition. We prepared 48 *para*-substituted (R^1) phenyl[*para*-substituted (R^2) phenyl isocyanide]gold(I) complexes $\mathbf{R^1–R^2}$ (six R^1 and eight R^2 substituents) and then performed three-step screening experiments. The first screening step was selection of emissive complexes under UV light, which gave 37 emissive $\mathbf{R^1–R^2}$ complexes. The second screening step involved evaluation of the mechanochromic properties by emission spectroscopy. Twenty-eight complexes were found to be mechanochromic. The third screening step involved preparation of single crystals, reprecipitated powders, and ground powders of the 28 mechanochromic $\mathbf{R^1–R^2}$ complexes. The changes in the powder diffraction patterns of these complexes induced by mechanical stimulation were investigated. Two compounds exhibited a crystal-to-crystal phase transition upon mechanical stimulation, including the previously reported **H–H**. Single crystals of the as-prepared and ground forms of the newly discovered $\mathbf{CF_3–CN}$ complex were obtained. Density functional theory calculations indicated that the mechano-induced red-shifted emission of $\mathbf{CF_3–CN}$ is caused by formation of aurophilic interactions. Comparison of the crystal structures of $\mathbf{CF_3–CN}$ with those of the other complexes suggests that the weaker intermolecular interactions in the as-prepared form are an important structural factor for the observed mechano-induced crystal-to-crystal phase transition.

INTRODUCTION

Luminescent mechanochromism is a phenomenon where solid and liquid crystalline materials change their photoluminescence properties upon applying mechanical stimulation such as grinding, ball-milling, and crushing.[1] These emission color changes are caused by changes in intermolecular interaction patterns through changes in the molecular arrangement in crystalline and liquid-crystalline materials. The optical responses of mechanochromic compounds reveal their potential applicability to sensing and recording devices. One of the pioneering luminescent mechanochromic compounds is the zinc complex reported by Kanesato in 2005.[2,3] In the last decade, the number of reports on luminescent mechanochromic organic and organometallic compounds has increased markedly, and more than 300 reports have now been published. Our group first contributed to this research field in 2008, where we reported a novel aryl(aryl isocyanide)gold complex with a reversible mechanochromic response.[4] Subsequently, mechanochromism of structurally related gold isocyanide complexes has been reported.[5]

A literature survey of the crystal structure changes of reported mechanochromic compounds indicates that crystal-to-amorphous phase transitions often take place upon applying mechanical stimulation to alter their emission properties (Figure 1a). This is intuitively understandable because mechanical forces are noncoherent and random stimuli on solids, and can therefore alter the integrity of ordered molecular arrangements. Several of our previously reported complexes also show luminescent mechanochromism caused by crystal-to-amorphous phase transitions upon mechanical stimulation.[4,6] For such amorphous ground forms, in many cases, it is difficult to investigate existing intermolecular interaction patterns, which are important to obtain insight into the underlying mechanism of mechanochromism. In contrast, for mechanochromic compounds exhibiting crystal-to-crystal phase transitions (Figure 1b), it is possible to obtain detailed crystal structures both before and after changes in the emission color by preparing the corresponding single crystals. However, such mechanochromic compounds are rare: <10% of reported mechanochromic compounds show crystal-to-crystal phase transitions.[5a,5c,7] In addition, detailed analysis of mechanical-stimulation-induced crystal structure changes will help to clarify why macroscopic mechanical stimulation initiates effective perturbation in microscopic molecular arrangements, which is currently unknown.[8]

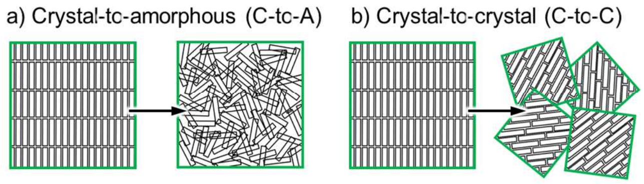

Figure 1. Schematic representations of typical solid-state structure changes of mechanochromic compounds (represented by black rectangles) upon applying mechanical stimulation.

Controlling the properties or behavior of mechanochromic compounds is challenging. Rational molecular design of mechanochromic compounds has hardly begun.[5d,9] Therefore, production of new mechanochromic compounds strongly relies on serendipitous discovery or derivatization of known mechanochromic compounds. For newly developed mechanochromic compounds, it is difficult to control their phase-transition behavior; i.e., change the profiles of crystal structures or optical properties. This is because mechanochromic behavior are related to the types of crystalline structures, and their control or engineering is known to be challenging.[10] Development of new strategies to produce mechanochromic compounds with desired properties and phase-transition behavior may advance investigation of mechanoresponsive luminescent materials.

We have intensively investigated aryl gold isocyanide complexes exhibiting a variety of intriguing mechanochromic properties.[4–6,7e] For example, a phenyl(phenyl isocyanide)gold complex (Figure 2, R^1 = R^2 = H)[5a,5e] and phenyl(dimethylphenyl isocyanide)gold complex[5b,5e] show mechano-induced single-crystal-to-single-crystal phase transitions with clear emission color changes, indicating the potential of this class of gold complexes. Both molecules also show typical mechanochromism upon strong grinding by ball-milling through crystal-to-crystal phase transitions (Figure 1b).[5a,7e] Although the molecular structures of these complexes are similar, the phase transition characteristics of these two complexes are contrasting.[5a,5b,5e,11] This indicates that the mechanochromic properties, including the emission properties, solid-state structures, and change in properties in response to mechanical stimulation, of aryl(aryl isocyanide) gold complexes strongly depend on the substituent patterns. We thus believe that systematic investigation of this family of complexes could uncover mechanochromic compounds with desired properties and behavior.

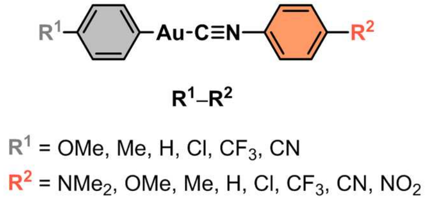

Figure 2. Structures of the 48 **R^1–R^2** complexes.

Here, we present a screening approach to discover mechanochromic compounds with desired behavior. We attempt to discover mechanochromic compounds with crystal-to-crystal phase transitions, which are an uncommon type of mechanochromic compound. The screening approach proposed in this work is based on three steps, as schematically illustrated in Figure 3. We prepare 48 gold(I) isocyanide complexes **R^1–R^2** by systematically changing the R^1 and R^2 substituents (Figure 2). We first screen the emission properties of these 48 **R^1–R^2** complexes under ultraviolet (UV) light (first screening, Figure 3), and find 37 emissive complexes. We then evaluate the emission color changes upon grinding by a spectroscopic technique (second screening, Figure 3). This gives 28 **R^1–R^2** complexes with prominent luminescent mechanochromism. To evaluate the profiles of the crystal structure changes of the 28 mechanochromic **R^1–R^2** complexes upon mechanical treatment, we perform powder and single-crystal X-ray diffraction (XRD) analyses (third screening, Figure 3). In addition to the previously reported **H–H** complex, we identify a new mechanochromic complex, **CF_3–CN**, exhibiting a crystal-to-crystal phase transition when its emission color changes upon mechanical stimulation. We further investigate the crystal structures, emission, and mechanochromic properties of the **CF_3–CN** complex to understand the mechanism of mechanochromism.

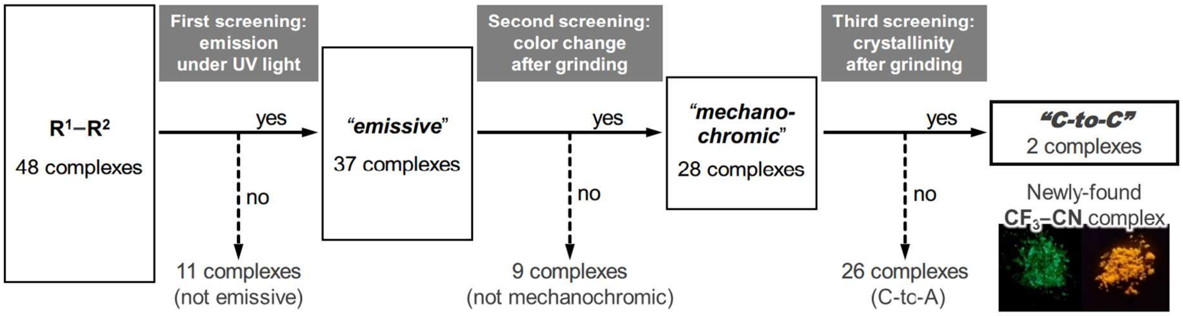

Figure 3. Schematic representation of the three-step screening approach used to identify mechanochromic compounds with crystal-to-crystal (C-to-C) phase transitions.

RESULTS AND DISCUSSION

Synthesis

We prepared 48 *para*-substituted phenyl(*para*-substituted phenyl isocyanide)gold(I) complexes **R^1–R^2** from fourteen precursors (Scheme 1). The **R^1–R^2** complexes were prepared by the reaction of *para*-substituted phenyl zinc compounds **1-R^1** (R^1 = OMe, Me, H, Cl, CF_3, and CN) and chloro(*para*-substituted phenyl isocyanide) gold(I) complexes **2-R^2** (R^2 = NMe_2, OMe, Me, H, Cl, CF_3, CN, and NO_2) in tetrahydrofuran (THF) at 0 °C (Scheme 1, see Supporting Information for more detail). The isolated yields of the **R^1–R^2** complexes ranged from 29% to 92%. The **1-R^1** compounds were prepared by the reaction of the corresponding *para*-substituted phenyl Grignard reagents and $ZnBr_2$, except for **1-CF_3** and **1-CN** compounds (see Supporting Information). **1-CF_3** and **1-CN** were prepared according to the procedure reported by Knochel, in which *para*-trifluoromethylphenyl iodide or *para*-cyanophenyl iodide, respectively, was reacted with Zn powder in the presence of LiCl.[12] The **2-R^2** compounds were prepared according to reported procedures[5a] from commercially available *para*-substituted aniline derivatives (see Supporting Information).

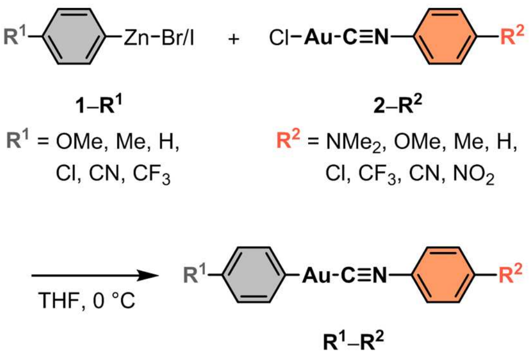

Scheme 1. Synthesis of the 48 **R^1–R^2** complexes.

Mechanochromic Properties

As a first screening step, we observed the photoluminescence of powder samples of the 48 **R^1–R^2** complexes. Eleven of the complexes were not emissive both before and after mechanical stimulation. We used as-prepared solid samples of the 48 **R^1–R^2** complexes as their unground forms, and their photographs were taken under UV illumination. We then ground the samples using a ball-mill at a rate of 4600 rpm for 15–30 min. Photographs of the resulting ground forms were then taken under UV illumination. These photographs are shown in Table 1, in which the powders on the left- and right-hand sides of each panel correspond to the as-prepared (unground) and ground samples of the **R^1–R^2** complexes, respectively (hereafter, the ground forms of the **R^1–R^2** complexes are referred to as **R^1–R^2_{ground}**). The ground and unground

Table 1. Photographs of the 48 **R^1–R^2** complexes under UV illumination. In each panel, unground and ground powders are on the left- and right-hand sides, respectively.

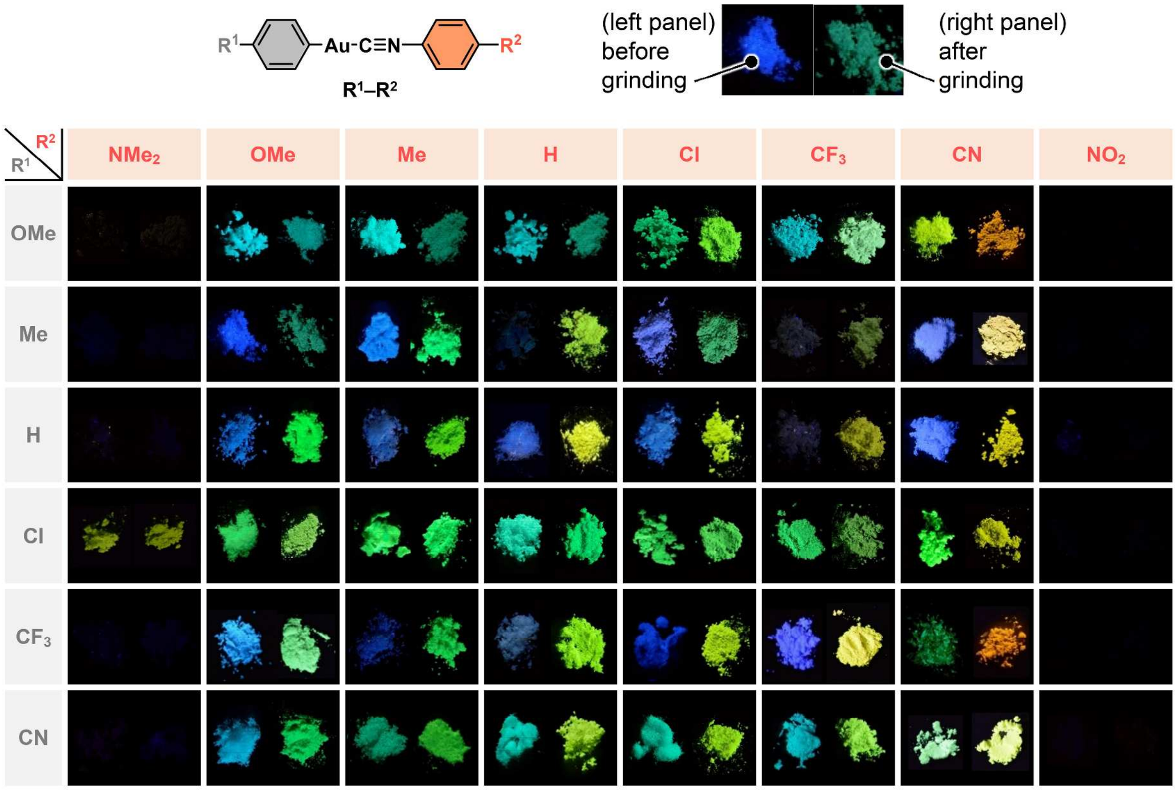

forms of **R^1–R^2** complexes containing NMe_2 and NO_2 groups as the R^2 moiety (**R^1–NMe$_2$** and **R^1–NO$_2$** complexes), excluding **Cl–NMe$_2$**, do not show photoluminescence in the visible region (left- and right-hand columns of Table 1). These complexes are mostly nonemissive, probably because of quenching through photoinduced electron transfer.[13] Thus, we conclude that these eleven complexes do not have mechanochromic properties. We used the other 37 **R^1–R^2** complexes in the second screening step.

We next evaluated the mechanochromic properties of the 37 luminescent **R^1–R^2** complexes by naked-eye observation under UV light and emission spectroscopy (second screening, Figure 3). The photographs in Table 1 reveal that most of these **R^1–R^2** complexes show clear emission color changes upon mechanical stimulation. We also measured excitation and emission spectra of the unground and ground forms of the **R^1–R^2** complexes (all of the spectra are summarized in Figure S1–S6 and Table S1). Based on the photographs under UV illumination (Table 1) and spectral shifts in the emission spectra of the as-prepared and ground **R^1–R^2** forms (Figure 4 and S1–S6), 28 complexes show mechanochromic properties. For example, the **H–OMe** complex is mechanochromic and shows an emission color change from blue to green upon ball-milling (Table 1). The emission maximum of the **H–OMe** complex upon excitation at 365 nm exhibits a red-shift from 429 to 522 nm (Figure 4a). As another example, the **OMe–CN** complex shows a green-to-yellow emission color change upon grinding (Table 1) and the emission maximum red-shifts by 60 nm (from 532 to 592 nm, Figure 4b). Similarly, the other 26 **R^1–R^2** complexes show emission color changes upon mechanical stimulation (Figure S1–S6).[14] Nine of the **R^1–R^2** complexes, **OMe–OMe**, **OMe–Me**, **OMe–H**, **Cl–NMe$_2$**, **Cl–OMe**, **Cl–Me**, **Cl–H**, **Cl–Cl**, and **Cl–CF$_3$**, show only very small spectral changes upon grinding (Figure S1 and S4). For example, the spectral changes of **Cl–Me** and **OMe–OMe** are shown in Figure 4c and d, respectively, in which the spectra are nearly the same. Indeed, emission color changes were not observed by the naked eye (Table 1). Thus, we determined that these nine complexes are not mechanochromic.[15] The remaining 28 mechanochromic **R^1–R^2** complexes were investigated in the third screening step.

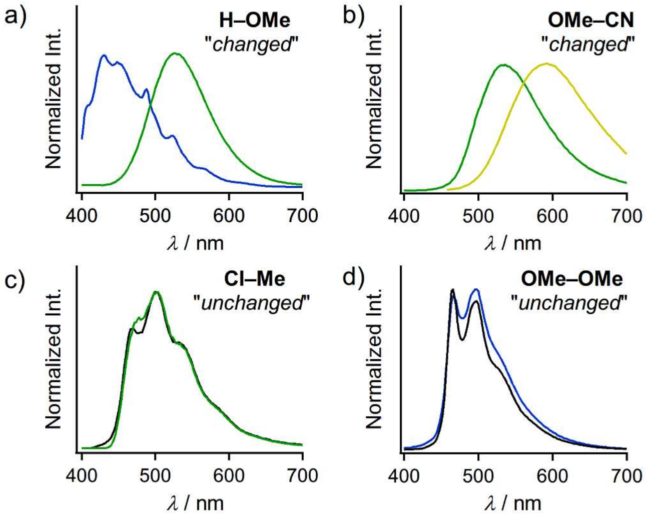

Figure 4. Emission spectra of (a) **H–OMe**, (b) **OMe–CN**, (c) **Cl–Me**, and (d) **OMe–OMe** following excitation at 365 nm. For (a), blue and green lines are the emission spectra of the unground and ground forms, respectively. For (b), green and yellow lines are the emission spectra of the unground and ground forms, respectively. For (c) and (d), colored and black lines are the emission spectra of the unground and ground forms, respectively.

Crystal Structure Changes

For the 28 mechanochromic **R^1–R^2** complexes, we performed a third screening: comparison of their molecular arrangements upon mechanochromism using XRD. To determine the mechanochromic **R^1–R^2** complexes with crystal-to-crystal phase transitions, we compared the powder XRD (PXRD) patterns before and after mechanical stimulation. If the **R^1–R^2** complexes show crystal-to-crystal phase transitions, the PXRD patterns before and after mechanical stimulation-induced emission color changes will be different. However, PXRD patterns of unground forms are difficult to obtain because unground forms are sensitive to mechanical stress applied during the measuring procedure of PXRD analysis. The mechano-sensitive nature of our complexes prevented placing the solid samples uniformly on substrates by pushing or pressing. Instead, in this study, we decided to use simulated powder patterns after single-crystal XRD analyses as the PXRD patterns of the unground forms of **R^1–R^2**. For **R^1–R^2$_{ground}$**, we can easily obtain diffraction patterns by typical PXRD measurements because these samples are mechanically insensitive.

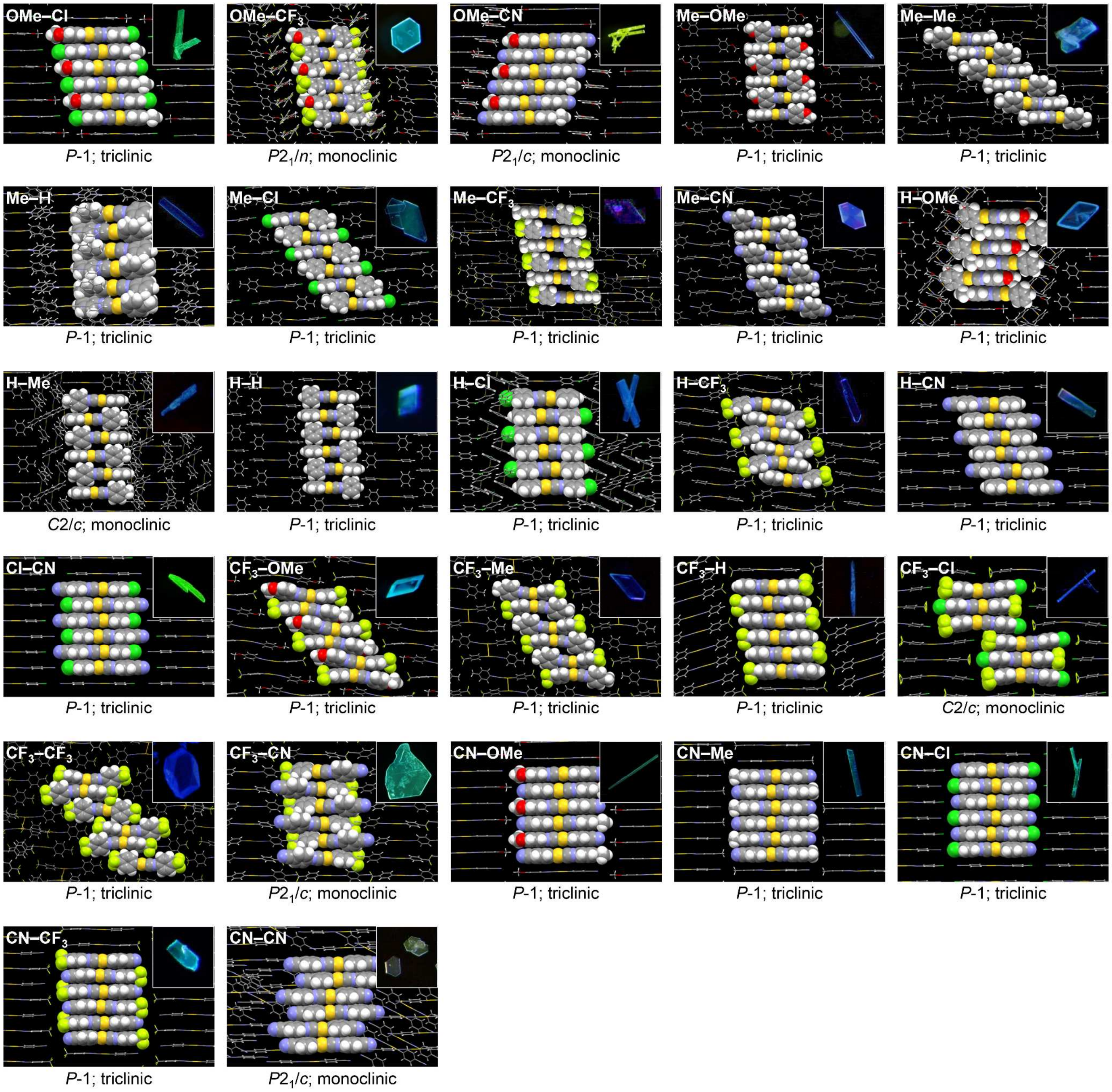

P-1; triclinic *P*2$_1$/*n*; monoclinic *P*2$_1$/*c*; monoclinic *P*-1; triclinic *P*-1; triclinic

P-1; triclinic *P*-1; triclinic *P*-1; triclinic *P*-1; triclinic *P*-1; triclinic

*C*2/*c*; monoclinic *P*-1; triclinic *P*-1; triclinic *P*-1; triclinic *P*-1; triclinic

P-1; triclinic *P*-1; triclinic *P*-1; triclinic *P*-1; triclinic *C*2/*c*; monoclinic

P-1; triclinic *P*2$_1$/*c*; monoclinic *P*-1; triclinic *P*-1; triclinic *P*-1; triclinic

P-1; triclinic *P*2$_1$/*c*; monoclinic

Figure 5. Crystal structures of the 27 single-crystal **R^1–R^2** complexes. The insets show photographs of the single crystals taken under UV illumination.

Recrystallization to prepare single crystals of the unground forms of the **R^1–R^2** complexes involved layering MeOH or hexane as a poor solvent on top of a solution of each **R^1–R^2** complex in CH_2Cl_2 (typically, 10 mg **R^1–R^2** in 1 mL CH_2Cl_2). Storing in a freezer for approximately 12 h gave crystal samples at the interface between the two solvents. After repeated trials, we obtained 27 single crystals for the 28 mechanochromic **R^1–R^2** complexes (Table S2). These single crystals were all of suitable quality for single-crystal analysis, as shown in Table S3 (R_1 values from 3.22% to 9.90%). For the **CN–H** complex, single-crystal analysis could not be performed because the crystals were too small and thin (Table S2). Instead, we prepared a reprecipitated powder of **CN–H** from CH_2Cl_2 and hexane and its PXRD pattern was recorded to gather information about the crystalline structure of the unground phase. The emission spectra of the single crystals and reprecipitated powders of the 28 complexes are almost the same as those of the powder samples (Figures S8–S12 and Tables S2 and S4). This indicates that the molecular arrangements of the **R^1–R^2** single crystals and reprecipitated powders are the same as those of the powder samples.[16] The space groups of these single crystals are mostly *P*-1 (nineteen single crystals), except for **OMe–CF$_3$** belonging to $P2_1/n$, **OMe–CN**, **CF_3–CN**, and **CN–CN** belonging to $P2_1/c$, and **H–Me** and **CF_3–Cl** belonging to $C2/c$. In the single-crystal structures (see the six molecules represented by the space-filling model in Figure 5), head-to-tail stacking with π-π stacking arrangements to form 1-D columns are typically observed. In some single crystals, such as **H–Me** and **H–H,** molecules have head-to-tail stacking with CH/π interactions (Figure 5). However, the molecules in **CF_3–CN** have a stacking-like arrangement with rotational displacement, indicating the presence of weak intermolecular interactions.[17]

Careful comparison of the simulated and PXRD patterns of the ground forms shows that most of the mechanochromic **R^1–R^2** complexes undergo crystal-to-amorphous phase transitions upon mechanical stimulation. For example, the simulated pattern of unground **CF_3–Cl** and the PXRD pattern of **CF_3–Cl_{ground}** are shown in Figure 6a. Clearly, the intensity of the diffraction pattern of **CF_3–Cl_{ground}** is low and different from that of the unground form, indicating that **CF_3–Cl_{ground}** is an amorphous phase. As another example, the diffraction patterns of **Me–Cl** are compared in Figure 6b. The peak positions of the diffractions of **Me–Cl_{ground}** (black line in Figure 6b) match well with those of the unground form (blue line in Figure 6b) even though the remaining peak intensity is relatively high. This may be caused by either the absence of a crystal structure change upon grinding or by the coexistence of the original crystal structure and a partially formed amorphous phase in the ground form. The former possibility is less likely than the latter because solid-state emission properties are typically strongly connected to the molecular arrangements in solid samples.[18,19] Instead, we consider that **Me–Cl** shows a crystal-to-(partial) amorphous phase transition when mechanical stimulation changes the emission properties. Indeed, mechanochromic compounds without complete phase transformation have been reported.[7e,19,20] As shown in Figure S13–S19, out of 28 **R^1–R^2** complexes, 26 **R^1–R^2** complexes show this type of change in their PXRD patterns upon grinding.[21] Only the **CF_3–CN** and **H–H** complexes do not fit into this category, which will be considered in the following paragraph.

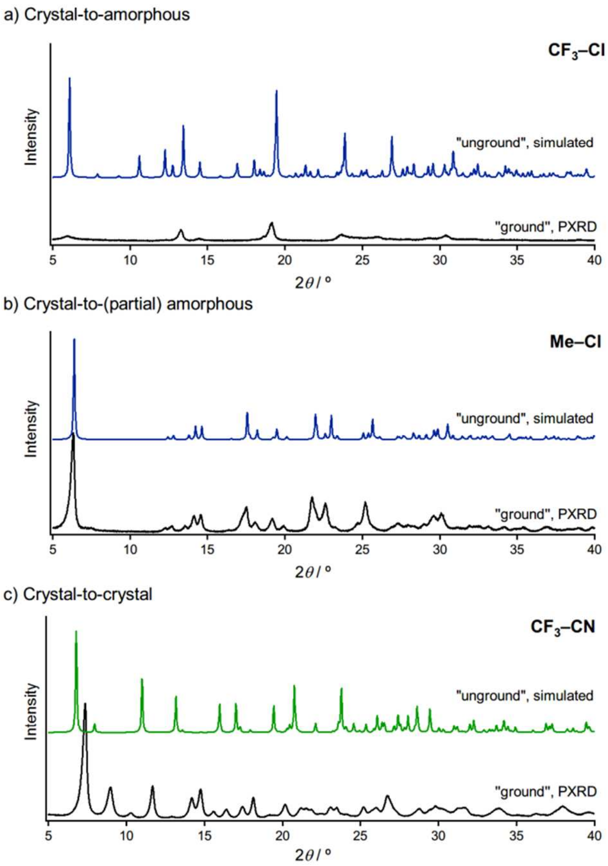

Figure 6. Simulated powder patterns of unground forms derived from single crystals (upper lines) and PXRD patterns of ground powders (lower lines) of (a) **CF_3–Cl**, (b) **Me–Cl**, and (c) **CF_3–CN** complexes.

In addition to the previously-reported **H–H** complex,[5a,5e] we discovered that **CF_3–CN** shows a crystal-to-crystal phase transition upon applying mechanical stimulation. Figure 6c depicts the simulated powder pattern of a **CF_3–CN** single crystal (green line) and PXRD pattern of the corresponding ground form (black line). The ground form of **CF_3–CN** exhibits an intense diffraction pattern in which the peak positions are different from those in the pattern of the unground form. This indicates that **CF_3–CN** undergoes a crystal-to-crystal phase transition upon mechanical grinding. As illustrated in Figure S15d, the previously reported **H–H** complex[5a] also exhibits different diffraction patterns before and after mechanical stimulation. These observations indicate that these two complexes show mechanochromism based on crystal-to-crystal phase transitions. Further discussion of the structural characteristics of these two crystals and comparison with other crystals is provided below. There are fewer than 20 reports of this type of crystal structure change for mechanochromic compounds.[5a,5c,7]

Mechanochromism of the CF_3–CN Complex

The changes in the optical properties of the **CF_3–CN** complex (Figure 7a) induced by grinding were investigated in more detail. Because the optical properties of the

H–H complex have already been reported in detail,[5a] we only investigated the **CF$_3$–CN** complex here. As shown in Figure 7b, the **CF$_3$–CN** complex displayed mechanochromism in which the green-emitting unground form transformed to a yellow-emitting ground powder after applying mechanical stimulation.[22,23] Figure 7c and d show excitation and emission spectral analyses of the **CF$_3$–CN** complex obtained before and after mechanical stimulation, respectively. Before grinding, the **CF$_3$–CN** complex exhibits a broad emission band centered at 510 nm (Figure 7d). After grinding, **CF$_3$–CN$_{\text{ground}}$** shows a 72-nm redshift and the emission maximum is at 582 nm. The excitation spectra of the **CF$_3$–CN** complex also show red-shifted bands following mechanical stimulation. The unground **CF$_3$–CN** complex shows a broad excitation spectral band up to 420 nm (green solid line in Figure 7c). After grinding, **CF$_3$–CN$_{\text{ground}}$** shows an excitation spectrum extending to 500 nm (yellow solid line in Figure 7c). We also confirmed that the average emission lifetime decreased (τ_{av}: from 47.1 to 0.756 μs) and the emission quantum yield increased (Φ_{em}: from 7.86 to 23.1%) upon mechanical stimulation (Figure S23 and Table S5).

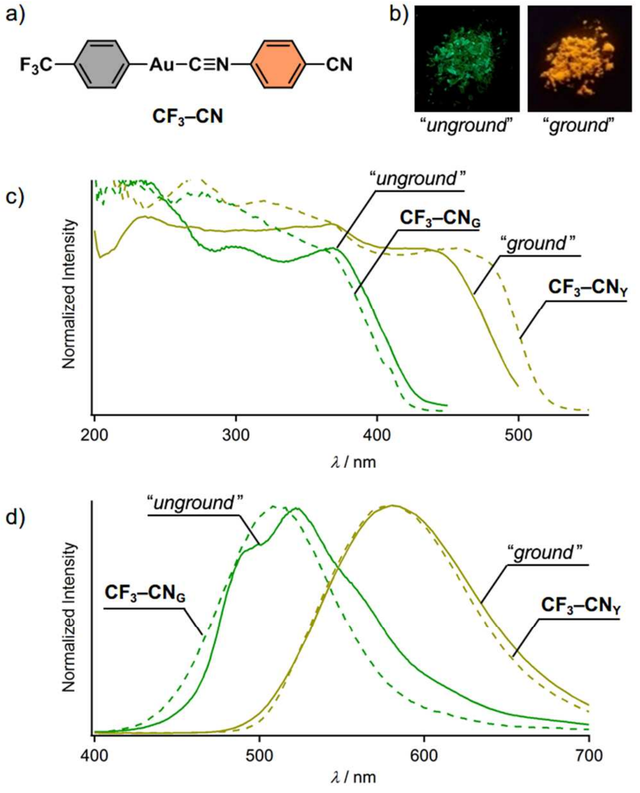

Figure 7. (a) Structure of the **CF$_3$–CN** complex. (b) Photographs of the unground and ground forms of the **CF$_3$–CN** complex taken under UV illumination. (c) Excitation spectra of powder samples of **CF$_3$–CN** before (solid green line, λ_{em} = 522 nm) and after (solid yellow line, λ_{em} = 582 nm) applying mechanical stimulation, and single crystals of **CF$_3$–CN$_\text{G}$** (dashed green line, λ_{em} = 510 nm) and **CF$_3$–CN$_\text{Y}$** (dashed yellow line, λ_{em} = 580 nm). (d) Emission spectra of powder samples of **CF$_3$–CN** before (solid green line) and after (solid yellow line) applying mechanical stimulation, and single crystals of **CF$_3$–CN$_\text{G}$** (dashed green line) and **CF$_3$–CN$_\text{Y}$** (dashed yellow line). λ_{ex} is 365 nm, except for **CF$_3$–CN$_\text{G}$** (λ_{ex} = 370 nm)

To determine the origin of the red-shifted emission band of the **CF$_3$–CN** complex upon grinding, the changes in the crystal structure were investigated in detail. Two different single crystals that correspond to the unground and ground forms of a material can provide molecular-level information about its crystal-to-crystal phase transition. Preparation of a single crystal of the unground form of **CF$_3$–CN** has already been described. Because this single crystal shows green emission (Figure 8a, i), hereafter, it will be referred to as **CF$_3$–CN$_\text{G}$**. The structural information obtained from the single crystal of **CF$_3$–CN$_\text{G}$** represents that of the unground powder form of **CF$_3$–CN** because they show similar characteristics in their excitation and emission spectra (Figure 7c and d, respectively). **CF$_3$–CN$_\text{G}$** crystallizes in monoclinic $P2_1/c$ space group [R_1 = 9.22%, wR_2 = 20.62%, GOF = 1.174, a = 16.125(2) Å, b = 22.172(3) Å, c = 7.618(1) Å, $\alpha = \gamma = 90°$, β = 95.115(4)°, Z = 8, V = 2712.8(7) Å^3, D_{calc} = 2.302 g cm^{-3}] (Table S3). Molecular layers are observed along the *ab* plane (Figure 8a, iv). Approximately perpendicular to this layer, molecules of **CF$_3$–CN$_\text{G}$** are arranged with slight rotational displacement without typical head-to-tail orientations (Figure 8a, ii and iii). Along this direction, molecules in the lattice only form very weak CH/π interactions (distance between H atom and centroid of the phenyl ring: 2.908 Å). Other typical intermolecular interactions in related single crystals of gold isocyanide complexes do not exist, such as π-π and aurophilic interactions.[5a,5b,24] It should be noted that the shortest Au···Au distance is 3.706 Å, which is much longer than the sum of the van der Waals radii of the Au atoms, indicating the absence of aurophilic interactions in **CF$_3$–CN$_\text{G}$**.

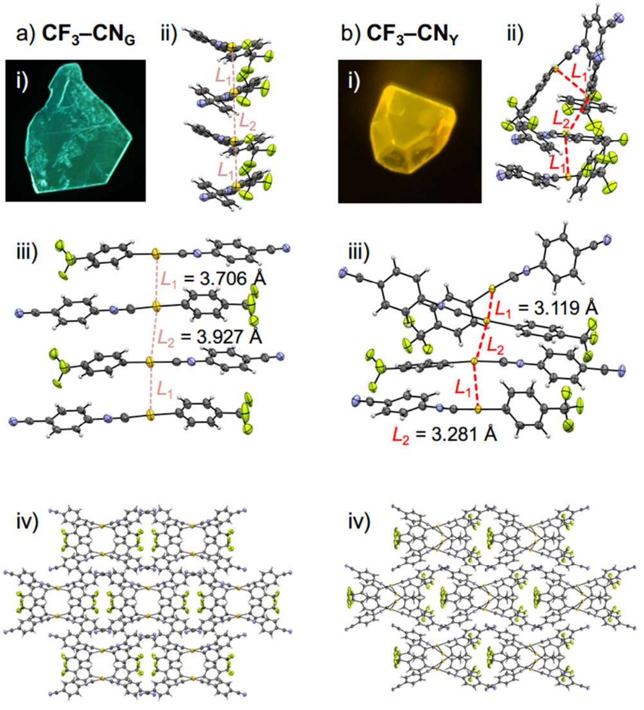

Figure 8. (i) Photographs taken under UV light and (ii)–(iv) single-crystal structures of (a) **CF$_3$–CN$_\text{G}$** and (b) **CF$_3$–CN$_\text{Y}$**.

We also prepared a yellow-emitting single crystal of **CF$_3$–CN$_Y$** by very slow crystallization (>1 day). Comparison of the powder patterns (Figure S25) and excitation/emission spectra (Figure 7c and d) of **CF$_3$–CN$_Y$** and **CF$_3$–CN$_{ground}$** indicates that the single crystal of **CF$_3$–CN$_Y$** corresponds to its ground form **CF$_3$–CN$_{ground}$**. **CF$_3$–CN$_Y$** crystallizes in orthorhombic $Pna2_1$ space group [R_1 = 4.82%, wR_2 = 13.84%, GOF = 1.063, a = 9.3279(4) Å, b = 19.4405(8) Å, c = 15.1865(8) Å, $\alpha = \beta = \gamma$ = 90°, Z = 8, V = 2753.9(2) Å^3, D_{calc} = 2.268 g cm^{-3}] (Table S3). Different from **CF$_3$-CN$_G$**, layer-like arrangements are not observed: the molecular arrangements of **CF$_3$–CN$_Y$** shown in Figure 8b iv diverge from one flat plane. Four derived molecules of **CF$_3$–CN$_Y$** are shown in Figure 8b ii and iii; they are almost randomly arranged without typical stacking arrangements. However, aurophilic interactions connect these molecules with Au···Au distances of 3.119 or 3.281 Å. All of these results indicate that upon mechanochromism of the **CF$_3$–CN** complex, a crystal-to-crystal phase transition occurs and aurophilic interactions are formed in the daughter phase.

Density functional theory (DFT) calculations based on the single-crystal structures of **CF$_3$–CN$_G$** and **CF$_3$–CN$_Y$** reveal that the red-shifted emission of **CF$_3$–CN** upon grinding is caused by the formation of new ordered crystalline structures containing aurophilic interactions. We performed time-dependent DFT (TD-DFT) calculations (B3LYP/SDD) of **CF$_3$–CN$_G$** and **CF$_3$–CN$_Y$** based on the tetramers derived from the single-crystal structures (Figure 9). The results indicate that the lowest unoccupied molecular orbital (LUMO) energy levels of **CF$_3$–CN$_G$** and **CF$_3$–CN$_Y$** are very similar (−3.13 and −3.10 eV, respectively). In contrast, the energy levels of the highest occupied molecular orbital (HOMO) are remarkably different (−6.88 and −6.30 eV, respectively). Destabilization of the HOMO energy level is typically observed in gold complexes with formation of aurophilic interactions.[25] The singlet excitation energy levels of **CF$_3$–CN$_G$** and **CF$_3$–CN$_Y$** obtained by TD-DFT calculations (B3LYP/SDD) also qualitatively match the experimental values (Figure S26). This indicates the underlying mechanism of luminescent mechanochromism of **CF$_3$–CN**: mechanical stimulation induces phase transition to a new crystal phase with aurophilic interactions, which induces the red-shifted emission band. We have previously reported structurally related arylgold(I) isocyanide complexes that exhibit red-shifted emission upon grinding because of the formation of new crystal structures with aurophilic interactions.[5a,5c] This mechanistic insight about the mechanochromism of **CF$_3$–CN** was obtained because single crystals of the unground and ground forms were able to be grown.

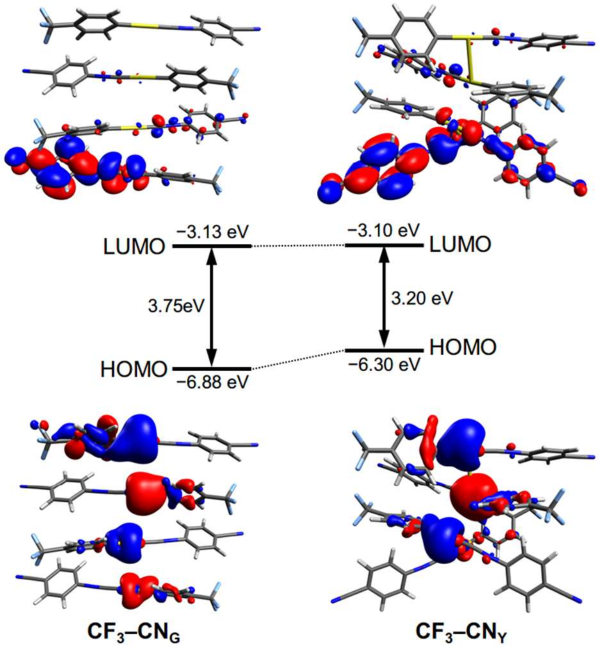

Figure 9. Frontier molecular orbitals and the corresponding energy potentials obtained by TD-DFT calculations of tetramers derived from the single-crystal structures of **CF$_3$–CN$_G$** and **CF$_3$–CN$_Y$**.

Structural Characteristic for Crystal-to-Crystal Phase Transitions

Through the present screening approach, we identified one structural characteristic of mechanochromic compounds with crystal-to-crystal phase transitions. As examples of molecular arrangements of unground **R^1–R^2**, the single-crystal structures of **CN–Me** and **CF$_3$–CN$_G$** are shown in Figure 10. **CN–Me** forms 1-D columns through π-π stacking interactions. Such molecular arrangements are often observed in other single crystals of **R^1–R^2** (Figure 5). In contrast, **CF$_3$–CN** (**CF$_3$–CN$_G$**) has molecular arrangements with a slight rotational displacement around the axis along the column direction. As a result, only a very weak CH/π interaction (distance between H atom and centroid of a phenyl ring: 2.908 Å) exists in **CF$_3$–CN$_G$**, and the rotational displacement prevents formation of other intermolecular interactions (π-π and aurophilic interactions). We carefully checked existing intermolecular interactions (CH/π, π-π, and aurophilic interactions) in the single-crystal structures of the 27 unground forms; the results are summarized in Table S6. Compared with **CF$_3$–CN$_G$**, the other 26 **R^1–R^2** single-crystal structures have more prominent intermolecular interactions, including CH/π, π-π, and/or aurophilic interactions, between neighboring molecules (Table S6). This suggests that the packing arrangement of **CF$_3$–CN$_G$** with relatively weak intermolecular interactions may be suitable for the mechano-induced phase transition to another crystal phase with stronger intermolecular interactions, such as **CF$_3$–CN$_Y$** with strong intermolecular interactions including aurophilic ones. These findings indicate that if such metastable crystalline arrangements with weak intermolecular interactions can be designed, we should be able to produce mechanochromic compounds with crystal-to-crystal phase transitions. One such example is a metastable dipolar amphiphile recently published by the research group including us.[7d] It should be noted that this is not the only structural requirement of mechanochromic compounds with crystal-to-crystal phase transitions because previously reported **H–H**[5a,5e] does not have this type of single-crystal structure (Figure 5). The unground phase of **H–H** forms head-to-tail dimers in the single crystal with prominent CH/π interactions (2.815 Å).

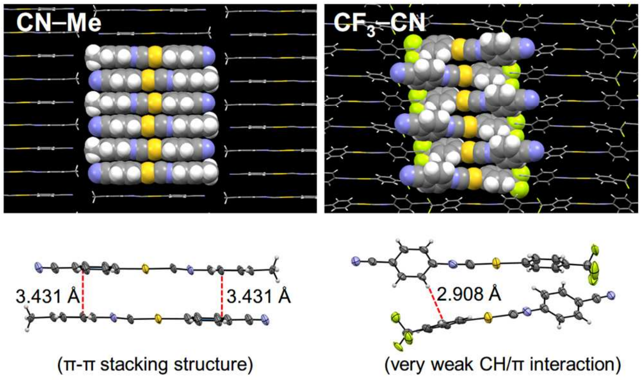

Figure 10. Comparison of the single-crystal structures of **CN–Me**, displaying π-π stacking interactions, and **CF_3–CN_G** showing rotational displacement.

The ground phases of both **CF_3–CN** and **H–H** complexes, which show crystal-to-crystal phase transitions, contain aurophilic interactions and are thermodynamically more stable than the corresponding unground phases. One similarity between the crystal structures of **CF_3–CN** and **H–H** is the formation of aurophilic interactions in the ground phases. Because aurophilic interactions are as strong as hydrogen-bonding interactions,[25] they can provide thermodynamic energy gain in the crystalline lattice after mechano-induced phase transitions of **CF_3–CN** and **H–H**. Indeed, differential scanning calorimetry analyses confirmed that the phase transitions of **CF_3–CN** (Figure S24) and **H–H**[5a,e] produced thermodynamically more stable phases. This is contrast to our previously reported gold complex displaying a mechano-induced crystal-to-amorphous phase transition in which mechanical stimulation produced a thermodynamically less stable phase.[4] In this study, we found eight **R^1–R^2** complexes that form aurophilic interactions in the unground phases (Table S6). These eight phases may be thermodynamically stable enough that there are no other crystal structures that are more stable; therefore, these complexes show crystal-to-amorphous phase transitions upon mechanochromism. These findings may indicate that thermodynamically stable molecular arrangements in unground phases of mechanochromic compounds are not suitable for crystal-to-crystal phase transitions.

SUMMARY

We prepared 48 gold isocyanide complexes **R^1–R^2** by reacting six *para*-substituted phenyl metal precursors **1-R^1** and eight chloro(*para*-substituted phenyl isocyanide) gold(I) **2-R^2**. The screening approach to find crystal-to-crystal phase transitions involved three screening steps. The first screening involved observing the photoluminescence of the complexes, and 37 **R^1–R^2** complexes were found to be emissive. The second screening involved applying mechanical stimulation to the 37 **R^1–R^2** complexes, and 28 **R^1–R^2** complexes were mechanochromic. For the 28 **R^1–R^2** complexes, single crystals, reprecipitated powders, and ground powders were prepared. We evaluated the changes in their diffraction patterns before and after mechanical stimulation (third screening). We found that two complexes, including the previously reported **H–H** complex, exhibited mechanochromism with crystal-to-crystal phase transitions. The mechanochromic properties of the second complex **CF_3–CN** were investigated in detail. Because we were able to obtain accurate information about the molecular arrangements of the unground and ground forms of **CF_3–CN**, we found that formation of aurophilic interactions induced red-shifted emission upon mechanical stimulation. By comparing the unground crystal structure of **CF_3–CN** and those of the other complexes, weaker intermolecular interactions were found in unground **CF_3–CN** than in the other complexes, which would be an important factor affecting its mechano-induced crystal-to-crystal phase transition. The insight obtained in this study will be useful for future design of this type of material. The present screening approach could be expanded to *ortho*- and *meta*-substituted gold isocyanide analogues, which would lead to development of mechanochromic compounds with unique properties, such as mechano-triggered single-crystal-to-single-crystal phase transitions.[5a,5b,5e,11] This work presents a promising screening approach for the discovery of mechanochromic materials with desired phase transitions/properties.

ASSOCIATED CONTENT

Supporting Information. Spectra, X-ray crystal graphics, thermal analyses, quantum chemical calculation data and other additional information. This material is available free of charge via the Internet at http://pubs.acs.org.

AUTHOR INFORMATION

Corresponding Author

seki@eng.hokudai.ac.jp; hajito@eng.hokudai.ac.jp

Present Addresses

Kita 13 Nishi 8 Kita-ku, Sapporo, Hokkaido, 060-8628, Japan

Author Contributions

All of the authors have given their approval to the final version of the manuscript.

ACKNOWLEDGMENT

This work was financially supported by the MEXT (Japan) program “Strategic Molecular and Materials Chemistry through Innovative Coupling Reactions” of Hokkaido University; Building of Consortia for the Development of Human

Resources in Science and Technology, "Program for Fostering Researchers for the Next Generation"; and by JSPS KAKENHI Grant Number 15H03804, 15K13633, and 26810042. We also thank the Frontier Chemistry Center Akira Suzuki “Laboratories for Future Creation” Project, Hokkaido University.

REFERENCES

(1) (a) Sagara, Y.; Kato, T. *Nat. Chem.* **2009**, *1*, 605–610; (b) Balch, A. L. *Angew. Chem. Int. Ed.* **2009**, *48*, 2641–2644; (c) Sagara, Y.; Yamane, S.; Mitani, M.; Weder, C.; Kato, T. *Adv. Mater.* **2016**, *28*, 1073–1095.

(2) Mizukami, S.; Houjou, H.; Sugaya, K.; Koyama, E.; Tokuhisa, H.; Sasaki, T.; Kanesato, M. *Chem. Mater.* **2005**, *17*, 50–56.

(3) Decreased intensity of solid-state photoluminescence upon mechanical grinding has been reported, see: Lee, Y. A.; Eisenberg, R. *J. Am. Chem. Soc.* **2003**, *125*, 7778–7779.

(4) Ito, H.; Saito, T.; Oshima, N.; Kitamura, N.; Ishizaka, S.; Hinatsu, Y.; Wakeshima, M.; Kato, M.; Tsuge, K.; Sawamura, M. *J. Am. Chem. Soc.* **2008**, *130*, 10044–10045.

(5) (a) Ito, H.; Muromoto, M.; Kurenuma, S.; Ishizaka, S.; Kitamura, N.; Sato, H.; Seki, T. *Nat. Commun.* **2013**, *4*, 2009; (b) Seki, T.; Sakurada, K.; Ito, H. *Angew. Chem. Int. Ed.* **2013**, *52*, 12828–12832; (c) Seki, T.; Ozaki, T.; Okura, T.; Asakura, K.; Sakon, A.; Uekusa, H.; Ito, H. *Chem. Sci.* **2015**, *6*, 2187–2195; (d) Yagai, S.; Seki, T.; Aonuma, H.; Kawaguchi, K.; Karatsu, T.; Okura, T.; Sakon, A.; Uekusa, H.; Ito, H. *Chem. Mater.* **2016**, *28*, 234–241; (e) Seki, T.; Sakurada, K.; Muromoto, M.; Seki, S.; Ito, H. *Chem. Eur. J.* **2016**, *22*, 1968–1978.

(6) Kawaguchi, K.; Seki, T.; Karatsu, T.; Kitamura, A.; Ito, H.; Yagai, S. *Chem. Commun.* **2013**, *49*, 11391–11393.

(7) (a) Yoon, S.–J.; Chung, J. W.; Gierschner, J.; Kim, K. S.; Choi, M.–G.; Kim, D.; Park, S. Y. *J. Am. Chem. Soc.* **2010**, *132*, 13675–13683; (b) Harada, N.; Abe, Y.; Karasawa, S.; Koga, N. *Org. Lett.* **2012**, *14*, 6282–6285; (c) Abe, Y.; Karasawa, S.; Koga, N. *Chem. Eur. J.* **2012**, *18*, 15038–15048; (d) Yagai, S.; Okamura, S.; Nakano, Y.; Yamauchi, M.; Kishikawa, K.; Karatsu, T.; Kitamura, A.; Ueno, A.; Kuzuhara, D.; Yamada, H.; Seki, T.; Ito, H. *Nat. Commun.* **2014**, *5*, 4013; (e) Seki, T.; Sakurada, K.; Ito, H. *Chem. Commun.* **2015**, *51*, 13933–13936.

(8) As rare examples, mechano-induced emission color changes are known to be triggered by single-crystal-to-single-crystal phase transitions (see: references 5a, 5b, and 5e).

(9) (a) Han, T.; Zhang, Y.; Feng, X.; Lin, Z.; Tong, B.; Shi, J.; Zhi, J.; Dong, Y. *Chem. Commun.* **2013**, *49*, 7049–7051; (b) Li, G.; Song, F.; Wu, D.; Lan, J.; Liu, X.; Wu, J.; Yang, S.; Xiao, D.; You, J. *Adv. Funct. Mater.* **2014**, *24*, 747–753.

(10) (a) Braga, D.; Grepioni, F. *Chem. Soc. Rev.* **2000**, *29*, 229–238; (b) Mnyukh, Y. *Fundamentals of Solid-State Phase Transitions: Ferromagnetism and Ferroelectricity*; 1st Books Library: Miami, 2001; (c) Bernstein, J. *Polymorphism in molecular crystals*; Clarendon Press/International Union of Crystallography, Oxford University Press: New York, 2002; (d) Blagden, N.; Davey, R. J. *Cryst. Growth Des.* **2003**, *3*, 873–885; (e) Cruz-Cabeza, A. J.; Bernstein, J. *Chem. Rev.* **2014**, *114*, 2170–2191.

(11) Seki, T.; Ito, H. *Chem. Eur. J.* **2016**, *22*, 4322–4329.

(12) Krasovskiy, A.; Malakhov, V.; Gavryushin, A.; Knochel, P. *Angew. Chem. Int. Ed.* **2006**, *45*, 6040–6044.

(13) The excited states of luminophores containing amino- and nitrobenzene rings are often quenched through acceptor- and donor-excited photoinduced electron transfer, respectively, because of the strong electron-donating and -withdrawing abilities of the substituents. For an example of quenching of luminophores containing aminobenzene groups, see: (a) Seki, T.; Yagai, S.; Karatsu, T.; Kitamura, A. *J. Org. Chem.* **2008**, *73*, 3328–3335. For an example of quenching of luminophores containing nitrobenzene groups, see: (b) Ueno T., Urano Y., Kojima H., Nagano T. *J. Am. Chem. Soc.* **2006**, *128*, 10640–10641.

(14) In Figure S7, we summarized the changes in emission maximum wavelength ($\lambda_{\mathrm{em,max}}$) of 28 **$R^1$–$R^2$** complexes upon mechanical stimulation.

(15) For these nine non-mechanochromic complexes, repeated trials of reprecipitation and recrystallization were performed. We did not obtain any solid samples with emission colors different from those shown in Table 1.

(16) That the single crystals and reprecipitated powders correspond to unground phases is also supported by their mechanochromic nature: mechanical stimulation of these single crystals and reprecipitated powders changes their emission colors and the corresponding ground powders **R^1–R^2_{ground}** were obtained.

(17) Further detailed discussion of the molecular arrangements of **R^1–R^2** is not included here because the main purpose of the preparation of single crystals in this study is to obtain their simulated powder patterns.

(18) (a) Shimizu, M.; Hiyama, T. *Chem. Asi. J.* **2010**, *5*, 1516–1531; (b) Gierschner, J.; Park, S. Y. *J. Mater. Chem. C* **2013**, *1*, 5818–5832; (c) Varughese, S. *J. Mater. Chem. C* **2014**, *2*, 3499–3516.

(19) (a) Chen, F.; Zhang, J.; Wan, X. *Chem. Eur. J.* **2012**, *18*, 4558–4567; (b) Zhang, G.-F.; Wang, H.; Aldred, M. P.; Chen, T.; Chen, Z.-Q.; Meng, X.; Zhu, M.-Q. *Chem. Mater.* **2014**, *26*, 4433–4446; (c) Zhang, D.; Gao, Y.; Dong, J.; Sun, Q.; Liu, W.; Xue, S.; Yang, W. *Dyes Pigm.* **2015**, *113*, 307–311.

(20) To support the occurrence of the crystal-to-(partial) amorphous phase transition of these complexes, we observed the intensity changes in the PXRD patterns when the ball-milling time was extended. For example, the results obtained for **H–CF_3** are shown in Figure S20. Diffraction intensities of **H–CF_3** gradually decreased when ball-milling time was prolonged from 15 to 60 min without newly emerged diffraction peaks. This result indicates that the ground phase of **H–CF_3** contains original crystalline phase and some amorphous domains, and that the content of amorphous domains increased upon prolonged ball-milling. This partially formed amorphous phase should be responsible for the new emission properties of **H–$CF_{3\mathrm{ground}}$**.

(21) As mentioned above, we used a reprecipitated powder of **CN–H** rather than a single crystal to gather the

PXRD patterns of its unground form. Comparison of the diffraction patterns of unground and ground phases of **CN–H** indicates that this complex shows a crystal-to-amorphous phase transition (Figure S19a). We also confirmed that that reprecipitated powder indeed shows mechanochromism: its emission color changed from green to yellow.

(22) The solid-state emission properties of **CF$_3$–CN** are very different from those of its monomeric state in CH$_2$Cl$_2$ solution (Figure S21 and S22 and Table S5). This indicates that intermolecular interactions in the crystalline lattices of **CF$_3$–CN** strongly affect the optical properties of this complex in the solid phases; i.e., **CF$_3$–CN$_G$** and **CF$_3$–CN$_Y$**.

(23) We investigated the thermal phase change of the green-emitting powder of **CF$_3$–CN** and found that the thermal phase change into yellow-emitting **CF$_3$–CN** occurred at around 150 °C according to emission color change and DSC analysis (Figure S24). This observation indicates that the yellow-emitting phase of **CF$_3$–CN** (corresponding to its ground phase) is thermodynamically more stable than the green-emitting one. The yellow-emitting phase of **CF$_3$–CN** does not show a thermally induced reverse phase transition back to the original phase, which was confirmed by observation of photoluminescence and DSC analysis (Figure S24).

(24) Seki, T.; Kurenuma, S.; Ito, H. *Chem. Eur. J.* **2013**, *19*, 16214–16220.

(25) (a) Balch, A. L. *Gold Bull.* **2004**, *37*, 45–50; (b) Pyykko, P. *Angew. Chem. Int. Ed.* **2004**, *43*, 4412–4456; (c) Yam, V. W.; Cheng, E. C. *Chem. Soc. Rev.* **2008**, *37*, 1806–1813; (d) Schmidbaur, H.; Schier, A. *Chem. Soc. Rev.* **2008**, *37*, 1931–1951.

Table of Content